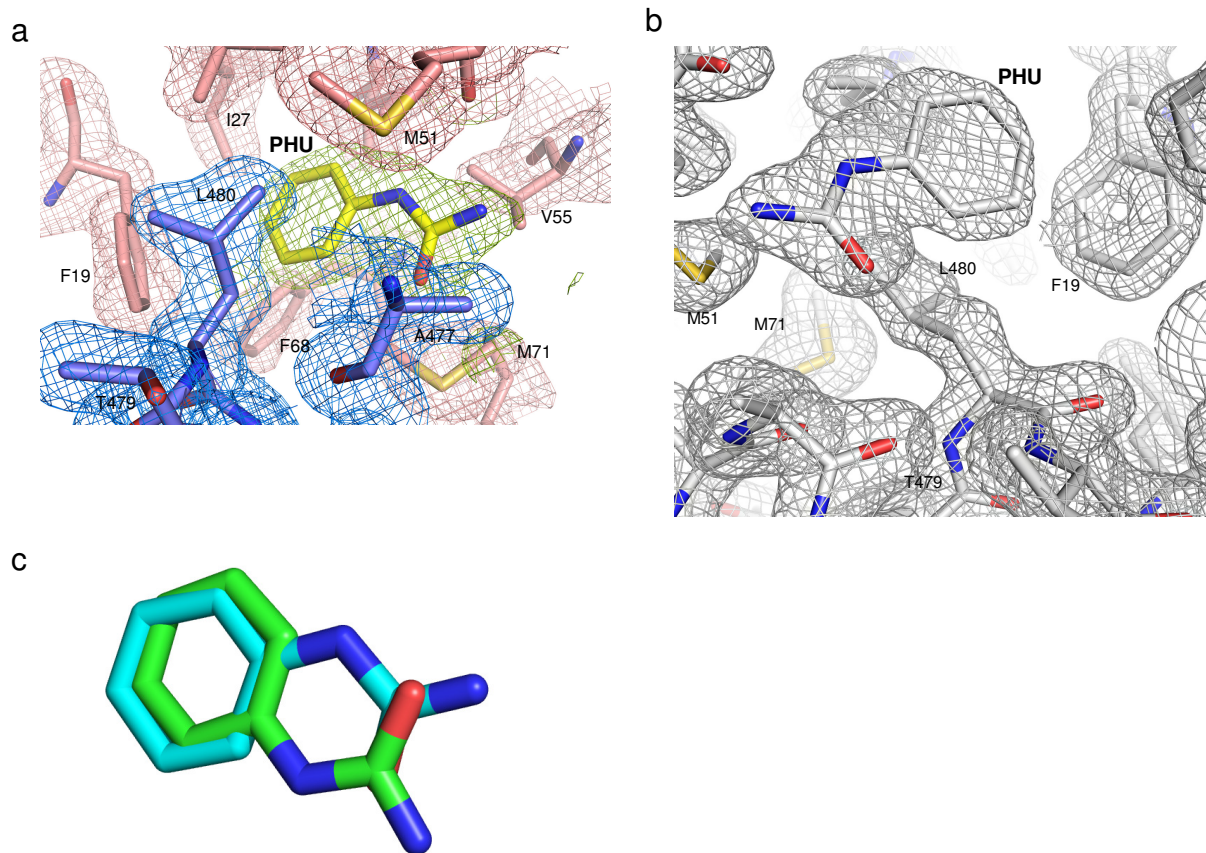
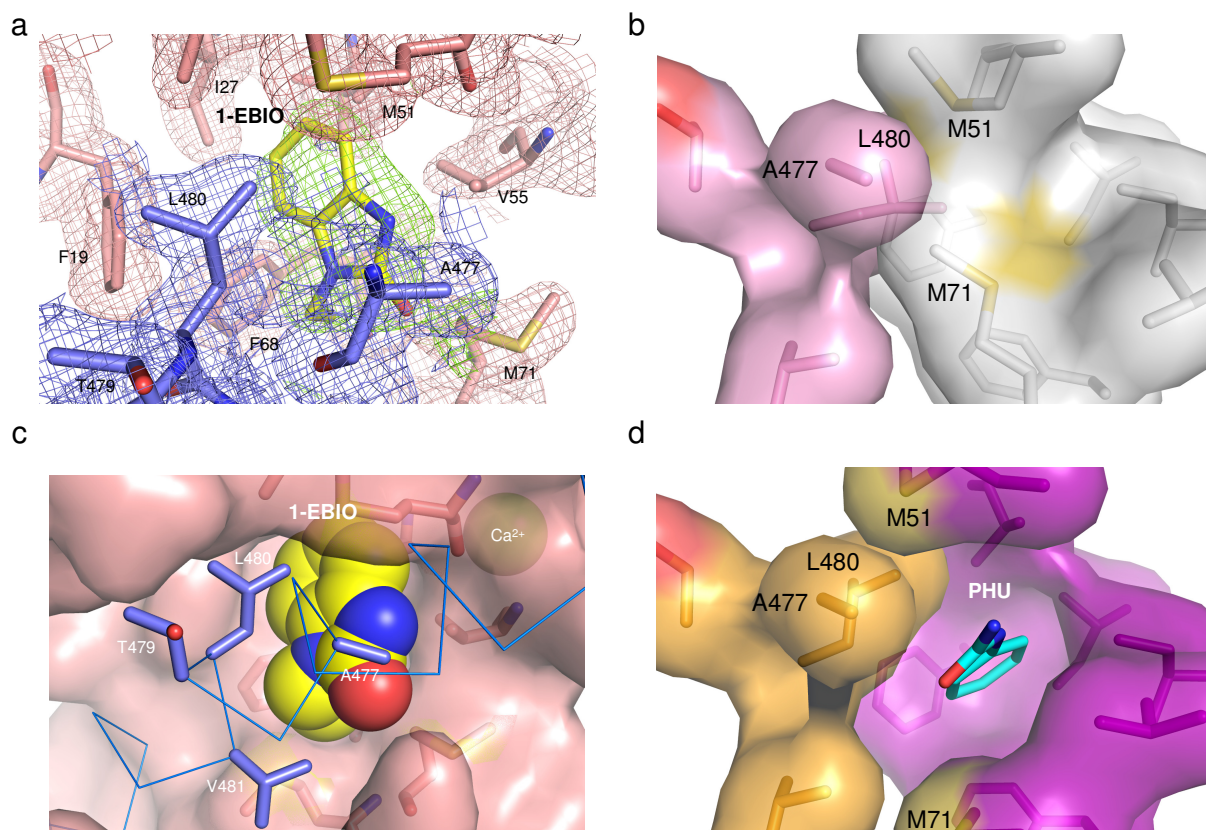


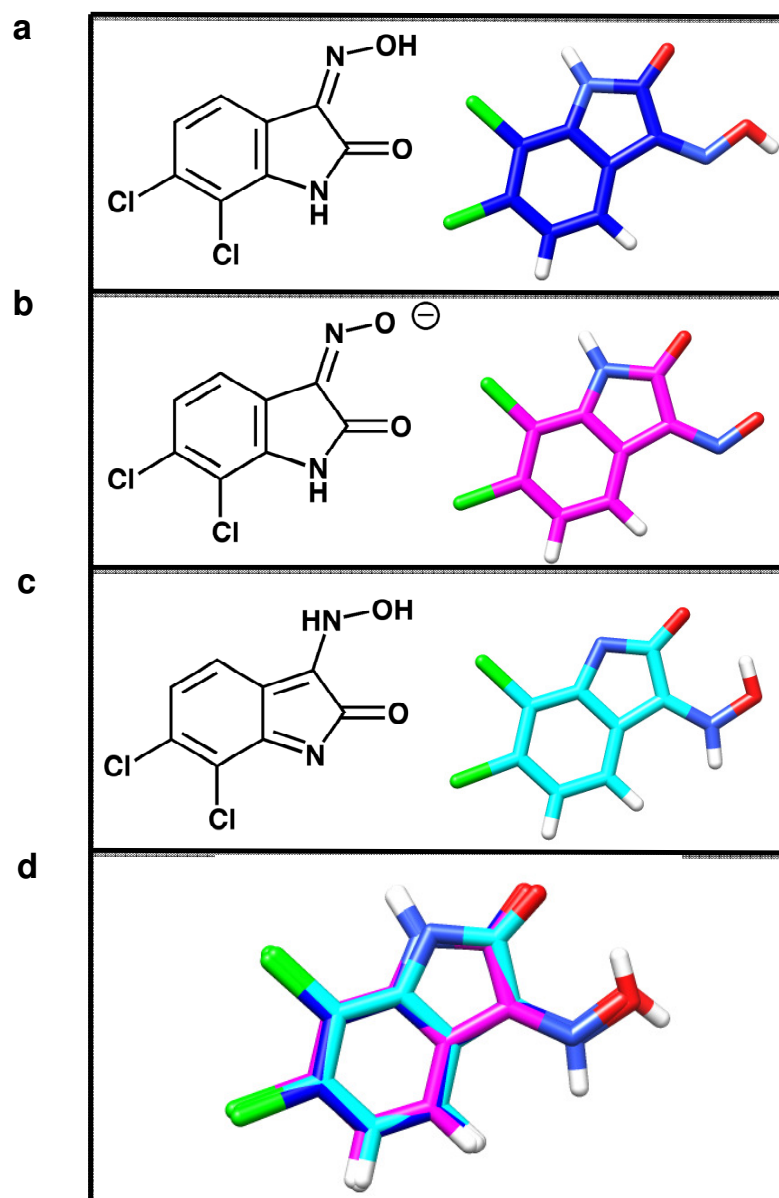
Supplementary Figures



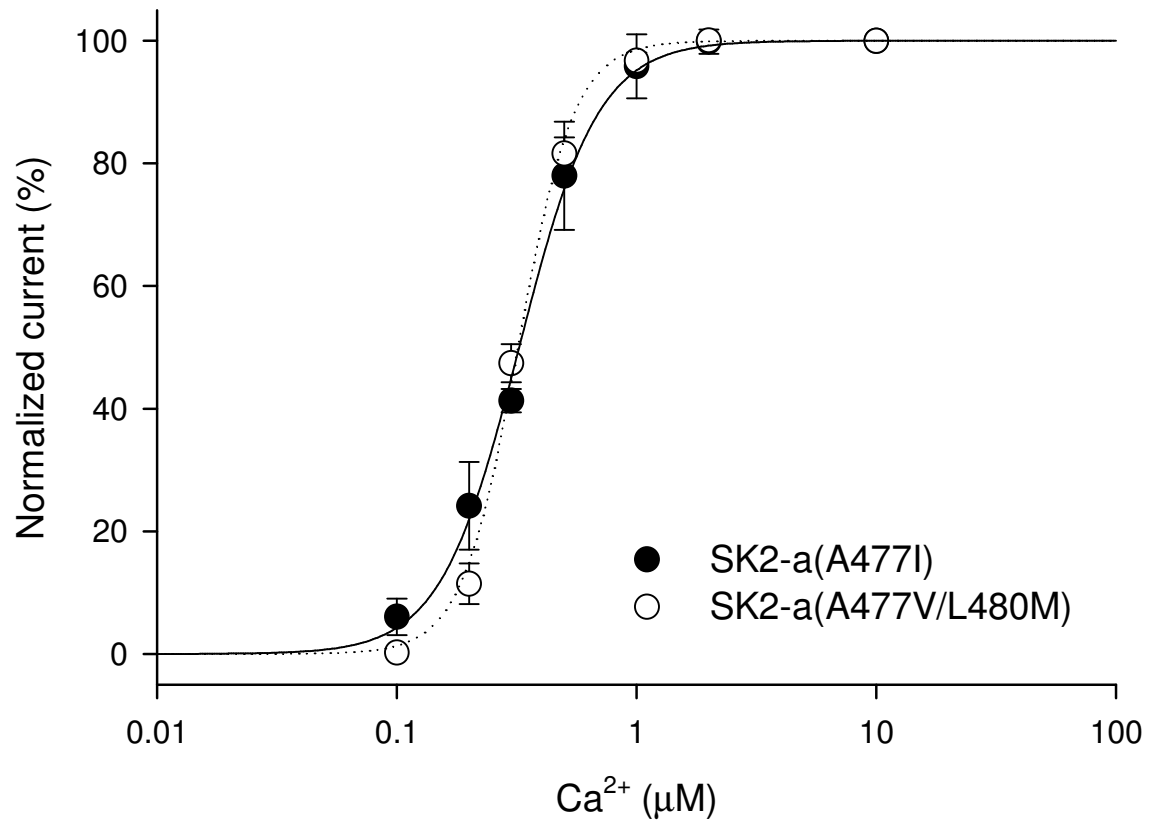
Supplementary Figure S1 | Location of PHU in the CaM-CaMBD2-b complex. (a) Electron density map constructed using 2mFo-DFc coefficients calculated in PHENIX⁶. The map is colored according to the subunit that is associated with the density: CaMBD2-b in blue, CaM in red, and PHU in yellow. The map is contoured at 1.2σ . The current refined model coordinates for residues in this region are drawn as sticks. Marine are amino acid residues from CaMBD2-a and salmon are amino acid residues from CaM. (b) A second view of the 2mFo-DFc electron density map in the vicinity of the PHU binding site with the current refined model coordinates overlaid. (c) Flip-flop of PHU in the PHU binding pocket.



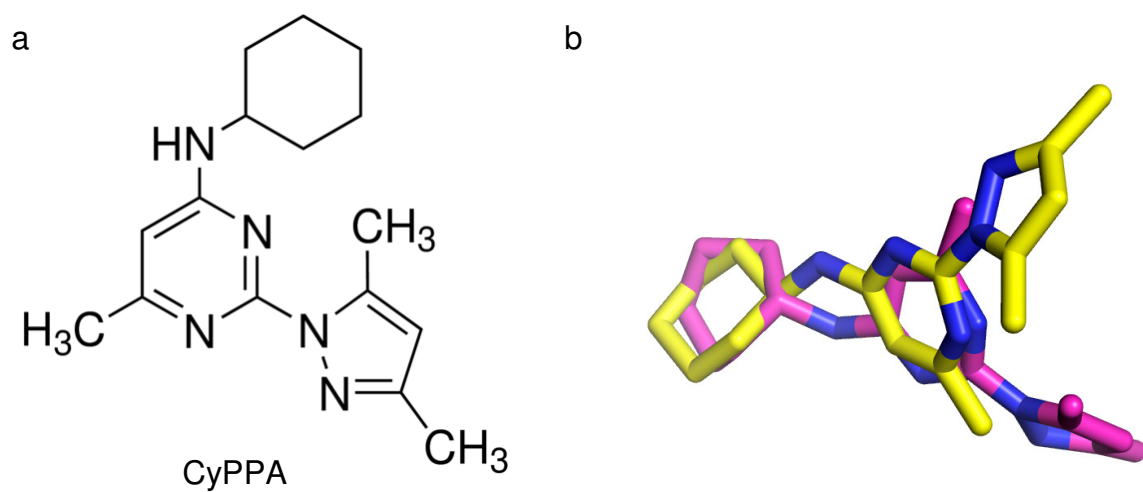
Supplementary Figure S2 | Formation of the 1-EBIO binding pocket at the CaM-CaMBD interface of the CaM N-lobe. (a) Electron density map constructed using 2mFo–DFc coefficients calculated in PHENIX⁶. The map is colored according to the subunit that is associated with the density: CaMBD2-b in blue, CaM in red, and 1-EBIO in yellow. The map is contoured at 1.2 σ . The current refined model coordinates for residues in this region are drawn as sticks. Marine are amino acid residues from CaMBD2-a and salmon are amino acid residues from CaM. (b) A space-filled model of the binding pocket for 1-EBIO at the CaM-CaMBD interface. Marine represents CaMBD and salmon represents CaM. (c) A space-filled model depicting the conformation, without the ligand, of the key amino acid residues which make up the binding pocket for both PHU and 1-EBIO (1G4Y). These amino acid residues include A477, T479, L480 and V481 from CaMBD (pink) and F19, I27, L32, M51, V55, I63, F68 and M71 of CaM (gray). Note that M71 interacts with both A477 and L480. (d) The same space-filled model in the presence of PHU, which also disrupts the interaction between M71 of CaM (purple) and A477/L480 of CaMBD (orange).



Supplementary Figure S3 | The NS309 tautomers have the same pose when docked in the pocket. There are three possible low energy tautomers of NS309 which are used for molecular docking. **(a)** The oxime tautomer of NS309, or the conventional tautomer from the literature. **(b)** The deprotonated oxime tautomer which may be favored at neutral pH. **(c)** The hydroxylamine tautomer of NS309 according to PUBCHEM and ZINC databases. In the binding mode of this tautomer, the amine NH forms a close interaction with the carbonyl group of M51 of CaM. **(d)** The lowest energy (consensus) binding mode from docking all of these tautomers, showing an excellent superposition of the conformations in the binding pocket. The predicted binding free energy of these different tautomers is also very similar, with the hydroxylamine being slightly more favorable.



Supplementary Figure S4 | No changes in Ca^{2+} dependent channel activation for the A477I and A477V/L480M mutants. Shown are the dose-response curves of the Ca^{2+} dependent activation of the A477I and A477V/L480M mutants expressed in TsA cells. The EC_{50} s, $0.33 \pm 0.03 \mu\text{M}$ ($n = 3$) and $0.32 \pm 0.01 \mu\text{M}$ ($n = 3$) respectively, are the same as the WT SK2-a channels as we previously reported². Data are mean \pm s.e.m..



Supplementary Figure S5 | CyPPA and its two potential conformations. (a) The chemical structure of CyPPA. (b) Predicted conformations of CyPPA in the CaM-CaMBD2-a complex of the WT (yellow) and A477V/L489M mutant (cyan), by molecular docking and MD simulations.